

## Electronic Supplementary Information

# Peptide-Assembly-Assisted Triplet-Triplet Annihilation Photon Upconversion in Non-deoxygenated Water

*Yajie Tian,<sup>a†</sup> Jieling Li,<sup>b†</sup> Luyang Zhao,<sup>b</sup> Xianglan Zhang,<sup>a</sup> Anhe Wang,<sup>b</sup> Honglei  
Jian,<sup>b</sup> Shuo Bai,<sup>b\*</sup> Xuehai Yan.<sup>b\*</sup>*

<sup>a</sup> School of Chemical and Environmental Engineering, China University of Mining and Technology (Beijing), Beijing 100083, China.

<sup>b</sup> State Key Laboratory of Biochemical Engineering, Institute of Process Engineering, Chinese Academy of Sciences, Beijing 100190, China.

<sup>†</sup> Yajie Tian and Jieling Li contributed equally to this work.

\* Corresponding author:

Prof. Shuo Bai, Email: [baishuo@ipe.ac.cn](mailto:baishuo@ipe.ac.cn)

Prof. Xuehai Yan, Email: [yanxh@ipe.ac.cn](mailto:yanxh@ipe.ac.cn)

KEYWORDS: short peptide; self-assembly; triplet-triplet annihilation upconversion; photosensitizer; nanostructure.

# Materials and methods

## 1. Materials

Fluorenylmethoxycarbonyl-Leucine (Fmoc-L),  
Fluorenylmethoxycarbonyl-Leucine-Leucine (Fmoc-L<sub>2</sub>),  
Fluorenylmethoxycarbonyl-Leucine-Leucine-Leucine (Fmoc-L<sub>3</sub>) and  
Fluorenylmethoxycarbonyl-Leucine-Leucine-Leucine-methoxyl (Fmoc-L<sub>3</sub>-OMe)  
were purchased from GL Biochem (Shanghai Ltd, China). Platinum(II)  
octaethylporphyrin (PtOEP) and 9,10-Diphenylanthracene (DPA) were purchased  
from Sigma-Aldrich (Shanghai Ltd, China). DMF was purchased from Beijing  
Chemical Works.

Millipore water was used throughout the study, with a resistivity of 18.2 MΩ cm<sup>-1</sup>.

## 2. Methods

### 2.1. Fabrication of peptide-UC chromophore co-assembled microrods

For the fabrication of Fmoc-L<sub>3</sub>/PtOEP/DPA co-assembled microrods, abbreviated hereafter as Fmoc-L<sub>3</sub> microrods, Fmoc-L<sub>3</sub> was first dissolved in DMF to obtain a transparent solution. For hydrophobic PtOEP and DPA, their complete dissolution in DMF was achieved by strong ultrasonic treatment at 40 °C, until two solutions became clear and transparent. Then the three solutions were mixed in different volumes to obtain the desired molar ratios. Finally, one volume of the above mixture was quickly added to 20 volume of water with gentle shaking and aged for at least 24 h to obtain the self-assembled microrods. All samples were washed by deionized water before characterizations. In the sequence control experiment, Fmoc-L<sub>3</sub> was replaced by same amount of Fmoc-L, Fmoc-L<sub>2</sub> and Fmoc-L<sub>3</sub>-OMe, respectively. The experimental method is the same as fabrication method of Fmoc-L<sub>3</sub> microrods.

### 2.2. Morphology characterization and elemental analysis of Fmoc-L<sub>3</sub> microrods

Morphology and composition of Fmoc-L<sub>3</sub> microrods were analyzed by scanning electron microscopy (SEM) and energy dispersion spectrum (EDS). At room temperature, an aliquot of a suspension of microrods was dropped on a silicon wafer and dried in vacuum. Before image acquisition and elemental analysis with an S-4800

(Hitachi, Japan, 10 kV voltage) instrument, the microrods on a silicon wafer were sputtered with carbon to increase conductivity. For transmission electron microscopy (TEM) observation by a JEOL JEM-1011 at 100 kV, a drop of sample carefully dropped to the carbon-coated copper grids and dried in vacuum.

### **2.3. Zeta potential measurement**

Zeta potential of samples was tested with Zetasizer (Malvern Instruments Ltd, Britain). Eight hundred and fifty microliters of the sample solutions were introduced into a DTS1070 folded capillary cell at 25.0 °C, and three measurements were performed and averaged for accuracy.

### **2.4. Spectra analysis of microrods**

UV-Vis and conventional photoluminescence spectra of samples in aqueous solution were recorded with a Shimadzu UV-2600 spectrophotometer and a fluorescence spectrometer (F-4500, Hitachi, Japan), respectively. The FTIR spectra were recorded on a Fourier transform infrared spectrometer (Brock Ltd, Hong Kong), from 4000 to 400  $\text{cm}^{-1}$  at room temperature. The sample was prepared by tablet method, and thirty-two scans were collected with a spectral resolution of 4  $\text{cm}^{-1}$ . The spectra of pure PtOEP and DPA carried out under the same conditions were used as control. A polarizing Optical Microscope (POM, Olympus BX53) was utilized to study the polarization properties of microrods. X-ray diffraction (XRD) pattern was performed on an Empyrean instrument (Panalytical, Netherlands).

### **2.5. Upconversion spectra of microrods measurement**

Upconverted emission intensity spectra of microrods were measured by femtosecond pulse laser (SP-5W, American Spectral Physics Corp, America) with an omni- $\lambda$  monochromator and a photomultiplier. The suspended sample in aqueous solution was excited at 532 nm with the collimated laser beam with a diameter of ca. 3 mm. Before upconversion spectra were recorded, the optical filter was used. Taking the average of 50 test data for all spectral curves and the deoxidized environment was produced by inert gas replacement.

### **2.6. Photoluminescence decay measurement (lifetime)**

Conventional photoluminescence decay traces were measured by FLS980. Fmoc-L<sub>3</sub>

microrods were excited at 532 nm and time-resolved single photon counting lifetime spectroscopy system was used (NanoLOG-TCSPC, Horiba Jobin Yvon, America) for measurement of upconversion decay traces. The quality of the fit has been judged by the fitting parameters as well as the visual inspection of the residuals.

### **2.7. The CLSM image of microrods**

An aliquot of a suspension of microrods was dropped on a glass slide and dried in vacuum at room temperature. Then at the mirror mode, confocal laser scanning microscopy (CLSM) images of the solid microrods were obtained by using an Olympus FV1000-IX81 instrument with a 60 oil-immersion objective (numerical aperture 1.4). Samples were excited with 559 nm laser and signals between 400 nm to 500 nm were collected to obtain upconverted CLSM image. Conventional CLSM images were obtained by 405 nm excited.

### **2.8. Measurement of TTA–UC relative quantum yield**

Herein, the upconversion relative quantum yield of Fmoc-L<sub>3</sub> microrods suspension was determined relative to the follow equation:

$$\phi_{UC} = 2\phi_{std} \left( \frac{A_{std}}{A_{UC}} \right) \left( \frac{I_{UC}}{I_{std}} \right) \left( \frac{\eta_{UC}}{\eta_{std}} \right)^2$$

Where  $\phi$  represents the quantum yield,  $A$ ,  $I$  and  $\eta$  represent the absorbance, integrated photoluminescence spectral profile and a refractive index of the solvent. The subscripts  $UC$  and  $std$  denote the parameters of the upconversion and standard systems. The quantum yield is generally defined as the ratio of emitted photon numbers to absorbed photon numbers, and thus the maximum value of theoretical calculation by multiplying two, by considering that the absorption of two photons is required for generating up-converted photon. This equation calculated the relative efficiency of TTA-UC and Rhodamine B in ethanol ( $\lambda_{ex}=550$  nm,  $\lambda_{em}=580$  nm,  $\phi_{std}=50\%$ ) was selected as the standard systems.

### **2.9. Molecular simulation**

The molecular dynamic (MD) simulation was performed using Gromacs (Version 5.1.4) package. The force field of Leu residue was used from Amber03, PtOEP fitted by MCPB.py,<sup>1</sup> and the rest residues generated by antechamber program in

Ambertools16 package and acpype.py program. The atomic charge of Leu residue was used from Amber03, and the rest atoms were fitted by DFT calculation under the restrained electrostatic potential (RESP) formalism and the resp program in Ambertools16. Water molecule was modeled using the tip3p potential.

The PtOEP-DPA binary system for MD simulation consisted of 2 PtOEP and 60 DPA in a water box sized  $8.0 \times 8.0 \times 8.0 \text{ nm}^3$ . The Fmoc-L<sub>3</sub>/PtOEP/DPA ternary system consisted of 2 PtOEP, 16 Fmoc-L<sub>3</sub>, and 60 DPA in the water box sized  $8.0 \times 8.0 \times 8.0 \text{ nm}^3$ . Both the binary and the ternary systems were firstly minimized utilizing the conjugate-gradient algorithm, and then equilibrated through running for 500 ps NVT simulations followed by 500 ps NPT simulations. Production runs in the NPT ensemble were then run for 150 ns at 300K and 1 bar, employing the leapfrog algorithm with a time step of 2 fs to integrate the equations of motion. The electrostatic forces were treated with the particle-mesh Ewald approach. Both the cutoff values of van der Waals forces and electrostatic forces were set to be 1.2 nm. The LINCS algorithm was utilized to preserve bonds.

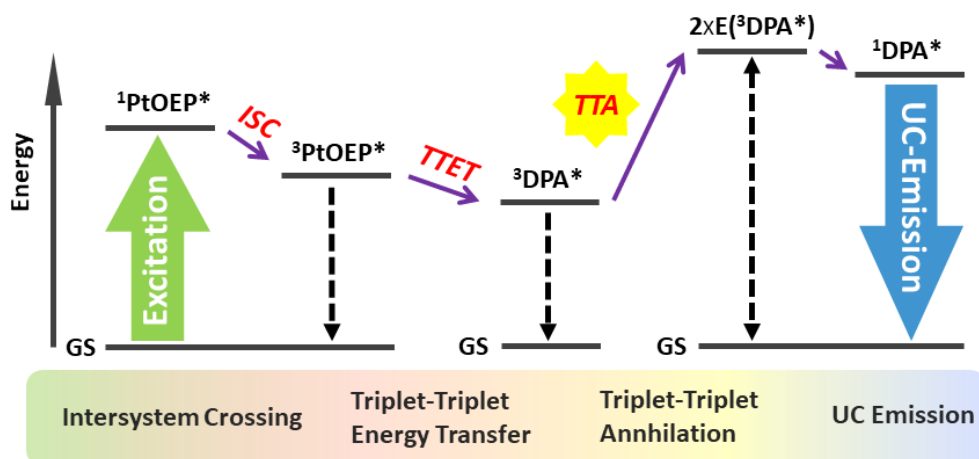
The DFT calculations were performed using *Gaussian 09 (Revision D.01)* package.<sup>2</sup> The molecular geometry was optimized at B3LYP/6-31G\* level.<sup>3</sup>

## References

- 1 P. Li, K. M. Merz, *J. Chem. Inf. Model.*, 2016, **56**, 599–604.
- 2 M. J. Frisch, G. W. Trucks, H. B. Schlegel, G. E. Scuseria, M. A. Robb, J. R. Cheeseman, G. Scalmani, V. Barone, B. Mennucci, G. A. Petersson, H. Nakatsuji, M. Caricato, X. Li, H. P. Hratchian, A. F. Izmaylov, J. Bloino, G. Zheng, J. L. Sonnenberg, M. Hada, M. Ehara, K. Toyota, R. Fukuda, J. Hasegawa, M. Ishida, T. Nakajima, Y. Honda, O. Kitao, H. Nakai, T. Vreven, J. A. Montgomery, J. J. E. Peralta, F. Ogliaro, M. Bearpark, J. J. Heyd, E. Brothers, K. N. Kudin, V. N. Staroverov, T. Keith,; R. Kobayashi, J. Normand, K. Raghavachari, A. Rendell, J. C. Burant, S. S. Iyengar, J. Tomasi, M. Cossi, N. Rega, J. M. Millam, M. Klene, J. E. Knox, J. B. Cross, V. Bakken, C. Adamo, J. Jaramillo, R. Gomperts, R. E. Stratmann, O. Yazyev, A. J. Austin, R. Cammi, C. Pomelli, J. W. Ochterski, R. L. Martin, K. Morokuma, V.

- G. Zakrzewski, G. A. Voth, P. Salvador, J. J. Dannenberg, S. Dapprich, A. D. Daniels, O. Farkas, J. B. Foresman, J. V. Ortiz, J. Cioslowski, D. J. Fox, Gaussian, Inc.: Wallingford CT, 2013.
- 3 A. D. Becke, *J. Chem. Phys.*, 1993, **98**, 5648–5652.

## Scheme and Figure



**Scheme S1.** The schematic diagram of TTA-UC mechanism.

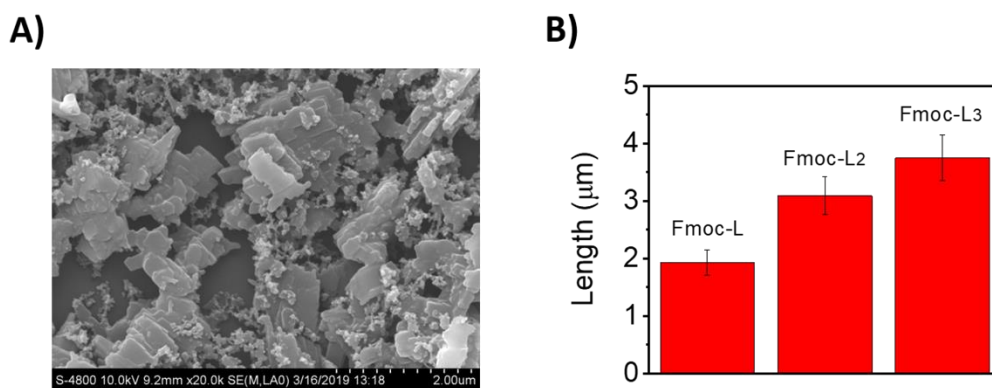


**Fig. S1** **A)** SEM image of PtOEP/DPA assembly in water; **B)** Length distribution of upconversion microrods with different short peptides.

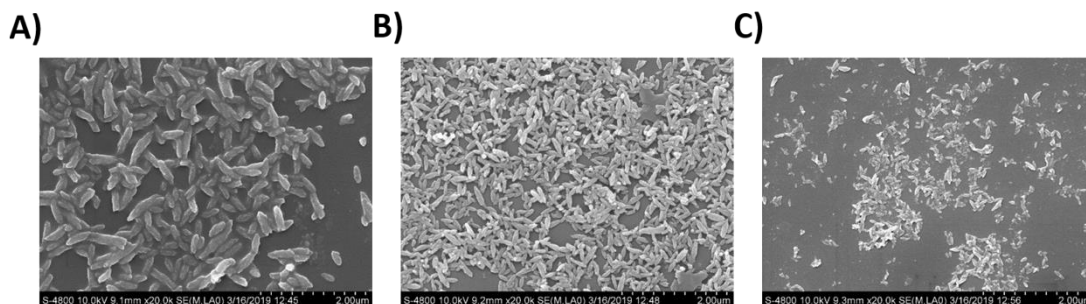


**Fig. S2** SEM images of peptides assembly in water. **A)** Fmoc-L<sub>1</sub>; **B)** Fmoc-L<sub>2</sub>; **C)** Fmoc-L<sub>3</sub>.

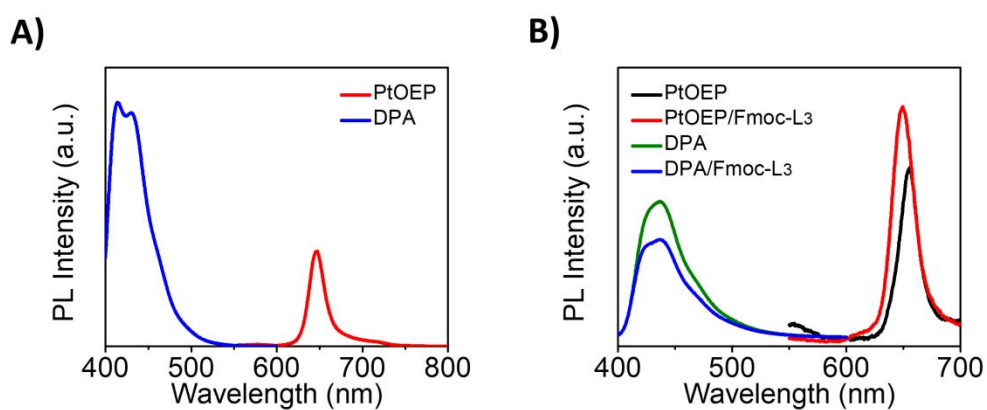


**Fig. S3** **A)** Conventional photoluminescence spectra of PtOEP and DPA in DMF; **B)** Conventional photoluminescence spectra of PtOEP, PtOEP/Fmoc-L<sub>3</sub>, DPA and DPA/Fmoc-L<sub>3</sub> in water.

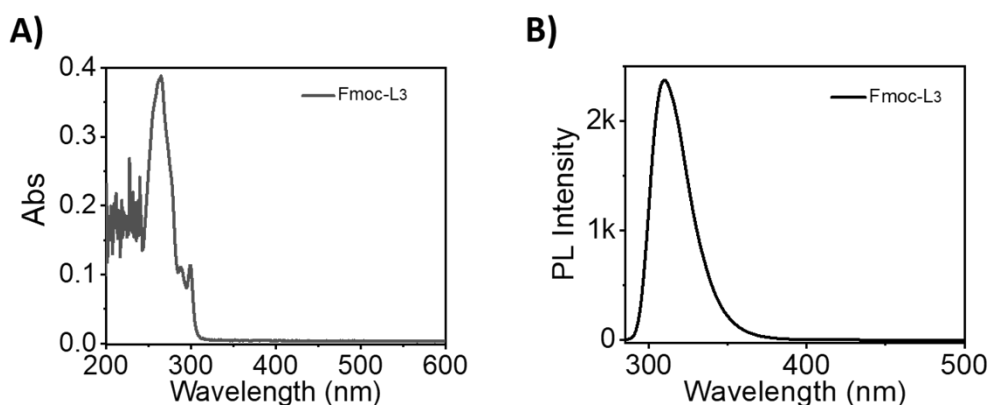


**Fig. S4** **A)** Absorption spectra of Fmoc-L<sub>3</sub> in water; **B)** Conventional photoluminescence spectra of Fmoc-L<sub>3</sub> in water.



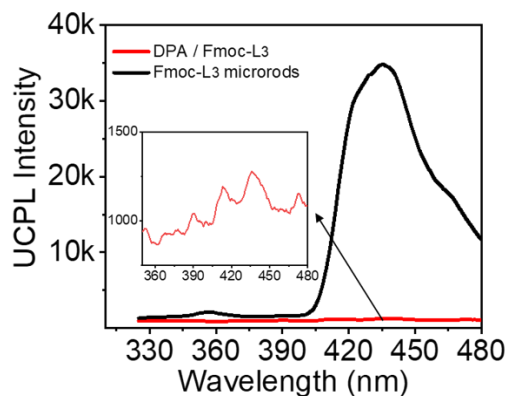


**Fig. S5** Upconversion photoluminescence spectra of DPA/Fmoc-L<sub>3</sub> and Fmoc-L<sub>3</sub> microrods (PtOEP=0.00867 mM, DPA=0.36 mM, Fmoc-L<sub>3</sub>=0.078 mM) in non-deoxygenated water under 532 nm excitation at the room temperature.

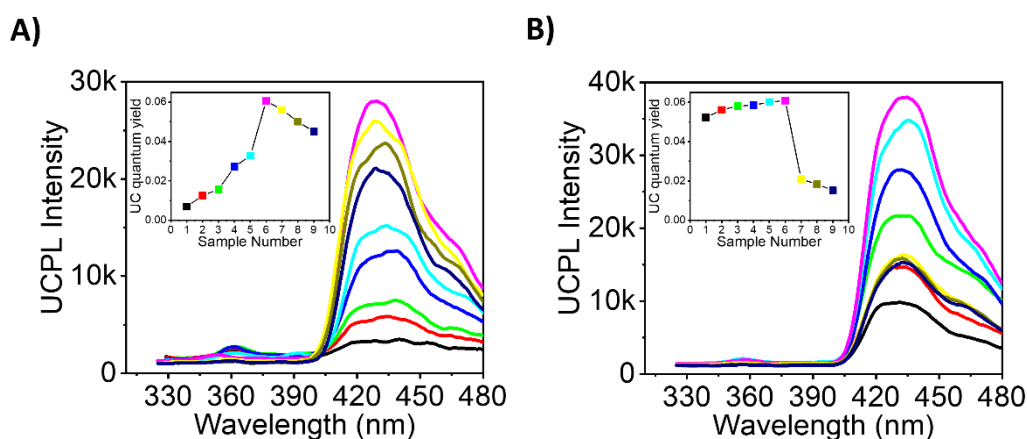


**Fig. S6** A) Upconversion photoluminescence spectra of Fmoc-L<sub>3</sub> microrods with different concentration of DPA (Fmoc-L<sub>3</sub>=0.1 wt%=0.0078mM, PtOEP=0.0052 mM, 1<sub>DPA</sub>=0.08 mM, 2<sub>DPA</sub>=0.12 mM, 3<sub>DPA</sub>=0.16 mM, 4<sub>DPA</sub>=0.20 mM, 5<sub>DPA</sub>=0.28 mM, 6<sub>DPA</sub>=0.36 mM, 7<sub>DPA</sub>=0.44 mM, 8<sub>DPA</sub>=0.52 mM, 9<sub>DPA</sub>=0.60 mM) in non-deoxygenated water under 532 nm excitation with 24 mW/cm<sup>2</sup>; B) Upconversion photoluminescence spectra of Fmoc-L<sub>3</sub> microrods with different concentration of PtOEP (Fmoc-L<sub>3</sub>=0.1 wt%=0.0078mM, DPA=0.36 mM, 1<sub>PtOEP</sub>=0.00086 mM, 2<sub>PtOEP</sub>=0.00170 mM, 3<sub>PtOEP</sub>=0.00350 mM, 4<sub>PtOEP</sub>=0.00520 mM, 5<sub>PtOEP</sub>=0.00694 mM, 6<sub>PtOEP</sub>=0.00867 mM, 7<sub>PtOEP</sub>=0.01040 mM, 8<sub>PtOEP</sub>=0.01214 mM, 9<sub>PtOEP</sub>=0.01387 mM) in non-deoxygenated water under 532 nm excitation with 24 mW/cm<sup>2</sup>. Inserted plots show the relationship between the UC efficiency and the mole ratio of chromophores.

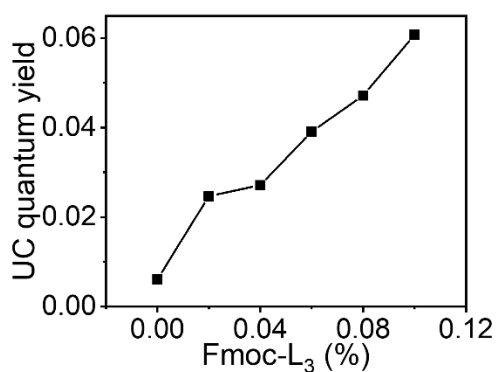


**Fig. S7** Line chart of UC efficiency and Fmoc-L<sub>3</sub> mass fraction. (PtOEP=0.00867 mM, DPA=0.36 mM).

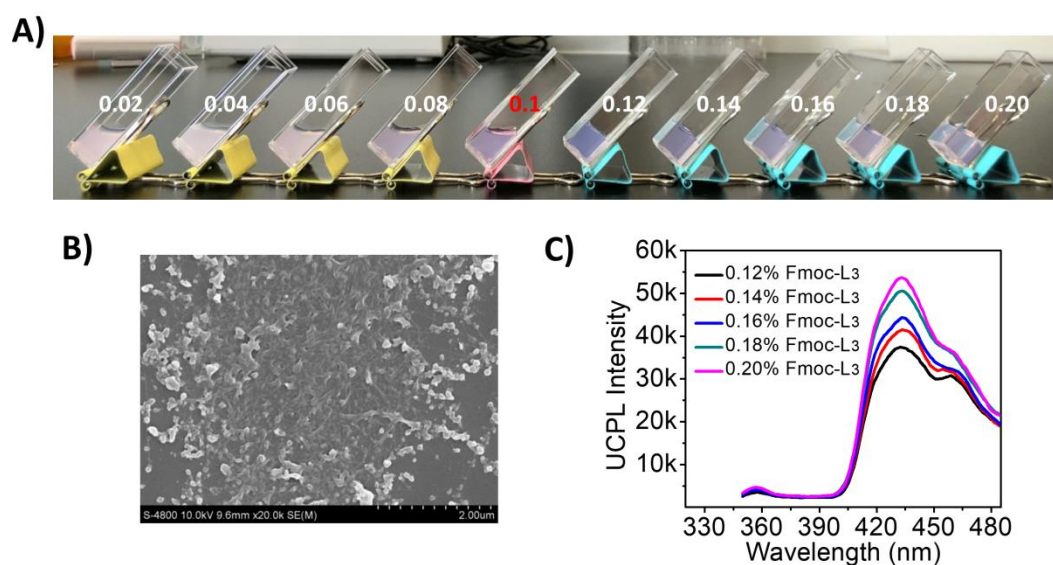


**Fig. S8** **A)** The photograph of Fmoc-L<sub>3</sub> ternary samples with different mass fraction of Fmoc-L<sub>3</sub> (0.02 wt%, 0.04 wt%, 0.06 wt%, 0.08 wt%, 0.10 wt%, 0.12 wt%, 0.14 wt%, 0.16 wt%, 0.18 wt%, 0.20 wt%) in aqueous phase; **B)** SEM image of hydrogel with 0.20 wt% Fmoc-L<sub>3</sub>; **C)** Upconversion photoluminescence spectra of hydrogels with different mass fraction of Fmoc-L<sub>3</sub>.

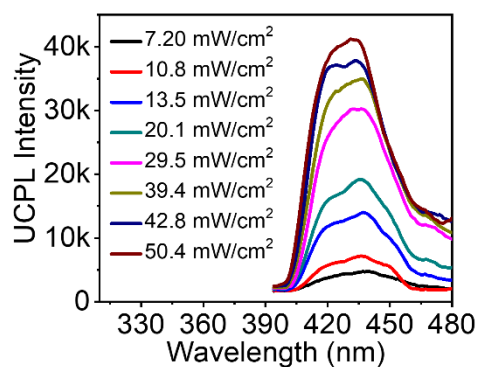


**Fig. S9** Upconversion photoluminescence spectra of Fmoc-L<sub>3</sub> microrods (PtOEP=0.00867 mM, DPA=0.36 mM, Fmoc-L<sub>3</sub>=0.078 mM) with different incident power density.

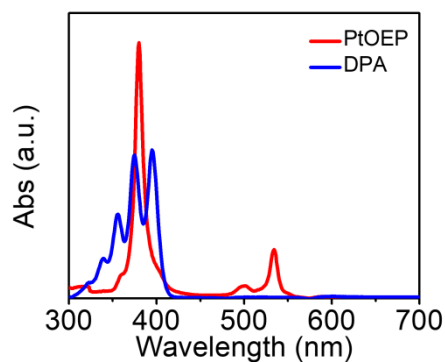


**Fig. S10** Absorption spectra of the PtOEP and DPA in DMF.

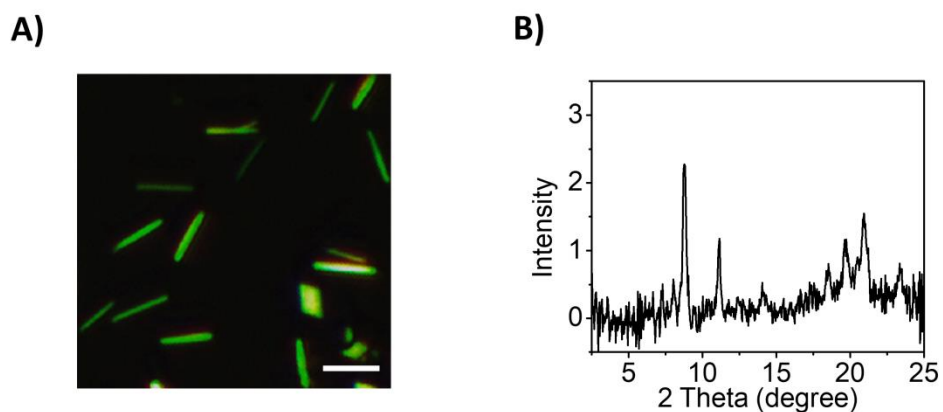


**Fig. S11** A) The polarizing microscope image of Fmoc-L<sub>3</sub> microrods (scale bar: 5  $\mu$ m); B) XRD spectrum of Fmoc-L<sub>3</sub> microrods.

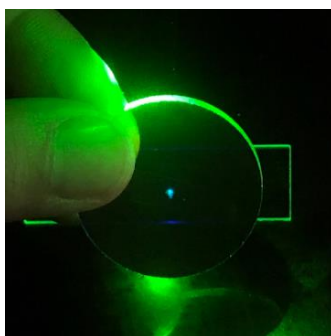


**Fig. S12** Upconversion luminescence image of Fmoc-L<sub>3</sub> microrods powder.